Available online at www.sciencedirect.com
ScienceDirect
ELSEVIER
Palaeogeography, Palaeoclimatology, Palaeoecology 240 (2006) 146–160
PALAEO
www.elsevier.com/locate/palaeo

Geochemical evidence for major environmental change at the Devonian–Carboniferous boundary in the Carnic Alps and the Rhenish Massif

Sandra I. Kaiser [a,1], Thomas Steuber [a,*], R. Thomas Becker [b], Michael M. Joachimski [c]

[a] *Institute of Geology, Mineralogy and Geophysics, Ruhr-University, 44801 Bochum, Germany*
[b] *Institute of Geology and Palaeontology, University of Münster, Corrensstr. 24, 48149 Münster, Germany*
[c] *Institute of Geology and Mineralogy, University of Erlangen, Schlossgarten 5, 91054 Erlangen, Germany*

Received 2 February 2005; accepted 24 March 2006

Abstract

A positive carbon isotope excursion is reported for the global Hangenberg Event near the Devonian–Carboniferous boundary, one of the most significant Phanerozoic mass extinction events. The $\delta^{13}C$ excursion occurs both in micritic limestones and in sedimentary organic matter of black shales and limestones from different palaeogeographical regions, which were precisely correlated by conodont biostratigraphy. The excursion indicates global change in the isotopic composition of marine dissolved inorganic carbon and atmospheric CO_2. This resulted from the increased burial of organic matter by globally widespread deposition of black shales.

The $\delta^{18}O$ values of conodont apatite indicate that globally widespread black shale deposition was preceded by increasing temperature, probably with a thermal gradient between equatorial and higher latitudes (~20 °S). The main regressive interval of the event, correlated previously with a short-lived glacial episode in Gondwana, yielded no material for geochemical analyses, but low temperatures are recorded in overlying beds and increase again during the terminal Devonian. Early Carboniferous sea-surface temperatures were similar to those of the Late Devonian.

This pattern of increased organic carbon burial, and changes in climate and sea level, is similar to that of several other extinction events of the Phanerozoic. It supports the hypothesis that increased organic carbon burial and oceanic anoxia can trigger mass extinctions, glaciations and eustatic sea-level change.

Keywords: Mass extinction event; Devonian–Carboniferous boundary; C isotopes; O isotopes; Conodonts; Apatite

1. Introduction

The Devonian–Carboniferous (D/C) boundary marks one of the major extinction events of the Phanerozoic, with a generic extinction rate exceeding 45% (Sepkoski, 1996). Shallow and deep-marine organisms, benthos (e.g., corals, bivalves and stromatoporoids), nekton (ammonoids, placoderms, conodonts), plankton (acritarchs, ostracods) as well as terrestrial ecosystems were

* Corresponding author. The Petroleum Institute, PO Box 2533, Abu Dhabi, United Arab Emirates. Tel.: +971 2 5085599.
E-mail addresses: kaiser.smns@naturkundemuseum-bw.de (S.I. Kaiser), tsteuber@pi.ac.ae (T. Steuber).
[1] Staatliches Museum für Naturkunde, Rosenstein I, D-70191 Stuttgart, Germany. Tel.: +49 711 8936 179.

0031-0182/$ - see front matter © 2006 Elsevier B.V. All rights reserved.
doi:10.1016/j.palaeo.2006.03.048

severely affected. Most extinctions occurred in the latest Famennian (Walliser, 1984) but a final extinction episode of a prolonged crisis interval is known from the basalmost Carboniferous (Becker, 1996). The main extinction took place at the top of the *Wocklumeria* Zone (UD VI-D) and within the Middle *praesulcata* Zone of the standard conodont zonation at the sudden change from oxygenated limestone (Wocklum Limestone) to anoxic shale facies (Fig. 1). It affected most strongly the ammonoids, wiping out all genera except for one prionoceratid genus and *Cymaclymenia* (Becker, 1996), the trilobites (no surviving species known, giving a cryptogenic ancestry of Carboniferous Proetida), conodonts, pelagic ostracods (e.g., Olempska, 1997) and deeper-water corals and bivalves. The major extinction of shallow water biota, such as stromatoporoids, biostromal corals, brachiopods and placoderms probably took place at the same time but neritic sections commonly display unconformities (e.g., Casier et al., 2005). A second smaller extinction occurred right at the Devonian–Carboniferous boundary, exterminating the last clymenid survivors and leading to a significant change of land plants, miospores and acritarchs (summary in Streel et al., 2000). A third extinction affected ammonoids just after they had started to recover in the basalmost Carboniferous (top of German Stockum level, top of globally widespread *Stockumites* Zone). The causal factors are still a matter of discussion (House, 2002) but published scenarios range from the impact of an extraterrestrial object (Bai, 1988; Wang et al., 1993), volcanism, fluctuations of sea level, oceanic anoxia (House, 1985; Becker, 1993), a climatic cooling episode (Streel et al., 2000), to changing patterns of oceanic circulation (Holser et al., 1996). Evidence for climate change is provided by latest Famennian glacial sediments in South America (e.g., Caputo, 1985; Isaacson et al., 1999; Streel et al., 2000) and South Africa (Almond et al., 2002), which were correlated with a major drop in sea level, the deposition of the Hangenberg Sandstone of the Rhenish Massif, and time-equivalent coarse-grained siliciclastics of Thuringia, SW England, Ireland, Portugal and North Africa (Sandberg et al., 1988; Becker, 1996). Contemporaneous glacial deposits may have also been deposited in western Africa and southern Libya (Streel et al., 2000). There are widespread unconformities at the Devonian–Carboniferous boundary on submarine seamounts and in shallow marine successions, for example, of Belgium (Casier et al., 2004), Pomerania, Poland (Matyja and Stempien-Salek, 1994), and the Russian Platform (Alekseev et al., 1994). This major polyphase and eustatically driven regression was preceded by a brief transgressive interval and the widespread deposition of black shales on the shelves of different continents. Biofacies (lack and extinction of benthos), pyrite levels and lack of bioturbation show that black shales were often deposited under anoxic conditions.

Previous geochemical analyses of boundary sections failed to record characteristic carbon isotope excursions at the D/C boundary in China (Xu et al., 1986) or in the Carnic Alps (Schönlaub et al., 1992, 1994). A positive excursion up to +7‰ δ^{13}C (PDB) was reported from brachiopods of the Latest Famennian Louisiana Limestone of Missouri (Brand et al., 2004). However, no correlation with the black shale deposits at the D/C boundary was established since the Louisiana Limestone falls in the Upper *praesulcata* Zone (Sandberg et al., 1972) which postdates both the initial transgressive black shale level and the subsequent major regression. Scott (1961) reported that *Protognathodus kockeli*, the defining species of the Upper *praesulcata* Zone, is one of the common species in the Louisiana Limestone. Chauffe and Nichols (1995) showed its presence in the lowest samples of the Louisiana Limestone at two sections. The base of the Louisiana Limestone is an unconformity surface and the main Hangenberg Event levels, especially the black shale interval, are not preserved. Brachiopods from the La Serre stratotype section of the Montagne Noire also produced rather positive carbon isotopic values (up to +5‰ δ^{13}C (PDB), Brand et al., 2004) but measured specimens were from Bed 82, which lies well above the black shale equivalent (Bed 69) and even above the subsequent main regressive interval (Beds 70 to 80, see facies analysis in Casier et al., 2002). Due to the lack of conodonts in the brachiopod-bearing Beds 82 to 83, it is impossible to decide whether they come from the top part of the Middle *praesulcata* Zone (as plotted in Brand et al., 2004) or from the Upper *praesulcata* Zone, which is first recorded in the overlying Bed 84 with the occurrence of *P. kockeli*. It is well possible that the La Serre and Louisiana Limestone brachiopods are contemporaneous (see possible deepening phase recognized by Casier et al., 2002 in Beds 81 to 84) and not from successive time intervals. The carbon isotope data of Brand et al. (2004) thus do not give insights into geochemical trends of the main phases of the Hangenberg Event but provided important evidence for elevated carbon isotopic values during the first, still topmost Devonian recovery interval within the extended crisis interval.

The present study focuses on the high-resolution correlation of geochemical records across a short time interval of probably less than 2 my, from the Late Famennian *expansa* to the Early Carboniferous *sandbergi* conodont zones (Fig. 1). The D/C boundary interval, equivalent to the multiphase Hangenberg Event as defined in the Rhenish

Massif (Walliser, 1984; Becker, 1993, 1996), begins at the base of the Middle *praesulcata* Zone (topmost Wocklum Limestone) and includes all beds up to the middle part of the *sulcata* Zone (base of the Hangenberg Limestone). The Hangenberg Black Shale corresponds to an initial sea-level highstand (maximum flooding) in the Middle *praesulcata* Zone and is followed by the Hangenberg Shale (highstand systems tract) and Hangenberg Sandstone. The latter reflects the main regressive phase of the event interval (lowstand systems tract), which grades into more shallow facies of the Seiler Conglomerate (an incised valley fill; see facies transect in Paproth, 1986). Miospores (LN Zone) provide a clear correlation between the main regressive phase and the glaciation pulse in Gondwana (Streel et al., 2000). A latest Famennian sea-level rise is recorded in the return to deeper pelagic sedimentation of the Stockum Limestone and lateral equivalents, including black shales and pyritic marlstones. The North American Louisiana Limestone also represents a relative deepening interval above an unconformity that separates it from the underlying top beds of the Saverton Shale, which contains pre-Hangenberg Event conodonts (Sandberg et al., 1972; see discussion in Chauffe and Nichols, 1995, p. 171–172). It correlates with the lower, topmost Devonian part of the Stockum Limestone (Bless et al., 1993). The first occurrence of the conodont *Siphonodella sulcata* within the *Stockumites* ammonoid Genozone (Becker, 1996) defines the D/C boundary. Due to the environment-controlled low abundance of oldest representatives of the index species in many sections, the boundary is alternatively drawn with the first occurrence of *Protognathodus kuehni* (Alberti et al., 1974).

Geochemical and biostratigraphical data are presented from D/C boundary sections (Fig. 2) at Grüne Schneid and Kronhofgraben (Schönlaub et al., 1992) in the Carnic Alps, and from Hasselbachtal (Rhenish Massif), a D/C boundary auxiliary stratotype (Becker and Paproth, 1993). Conodonts from stratigraphically well-defined levels were also analyzed from Oberrödinghausen (Rhenish Massif, see review of section in Luppold et al., 1994). Within the event interval, the lithofacies of the palaeo-equatorial Rhenish Massif (Fig. 1) are nodular limestones and siliciclastics deposited in a proximal shelf environment. Sections in the Carnic Alps consist of condensed pelagic cephalopod limestones deposited on a distal submarine rise in somewhat higher southern (~20° S) palaeolatitude.

2. Biostratigraphy

2.1. Carnic Alps

The faunal evolution and geochemical patterns of the condensed pelagic cephalopod limestones of the D/C boundary sections at Grüne Schneid and Kronhofgraben were investigated previously, but no characteristic

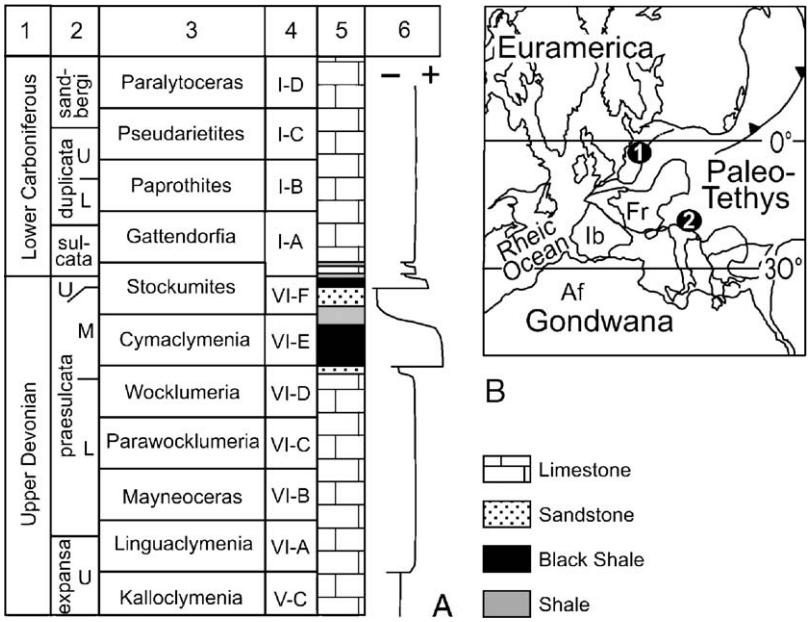

Fig. 1. (A) Stratigraphical correlation scheme used in the present study (updated after Becker, 1993, 1996) and (B) locality map. (A) 1, chronostratigraphy; 2, conodont biozonation; 3, ammonoid genozones; 4, ammonoid zonal keys; 5, generalized lithostratigraphy of D/C boundary sections in the Rhenish Massif; 6, sea-level change, modified after Bless et al. (1993). (B) 1, Rhenish Massif; 2, Carnic Alps; Af, Africa; Ib, Iberia; Fr, France.

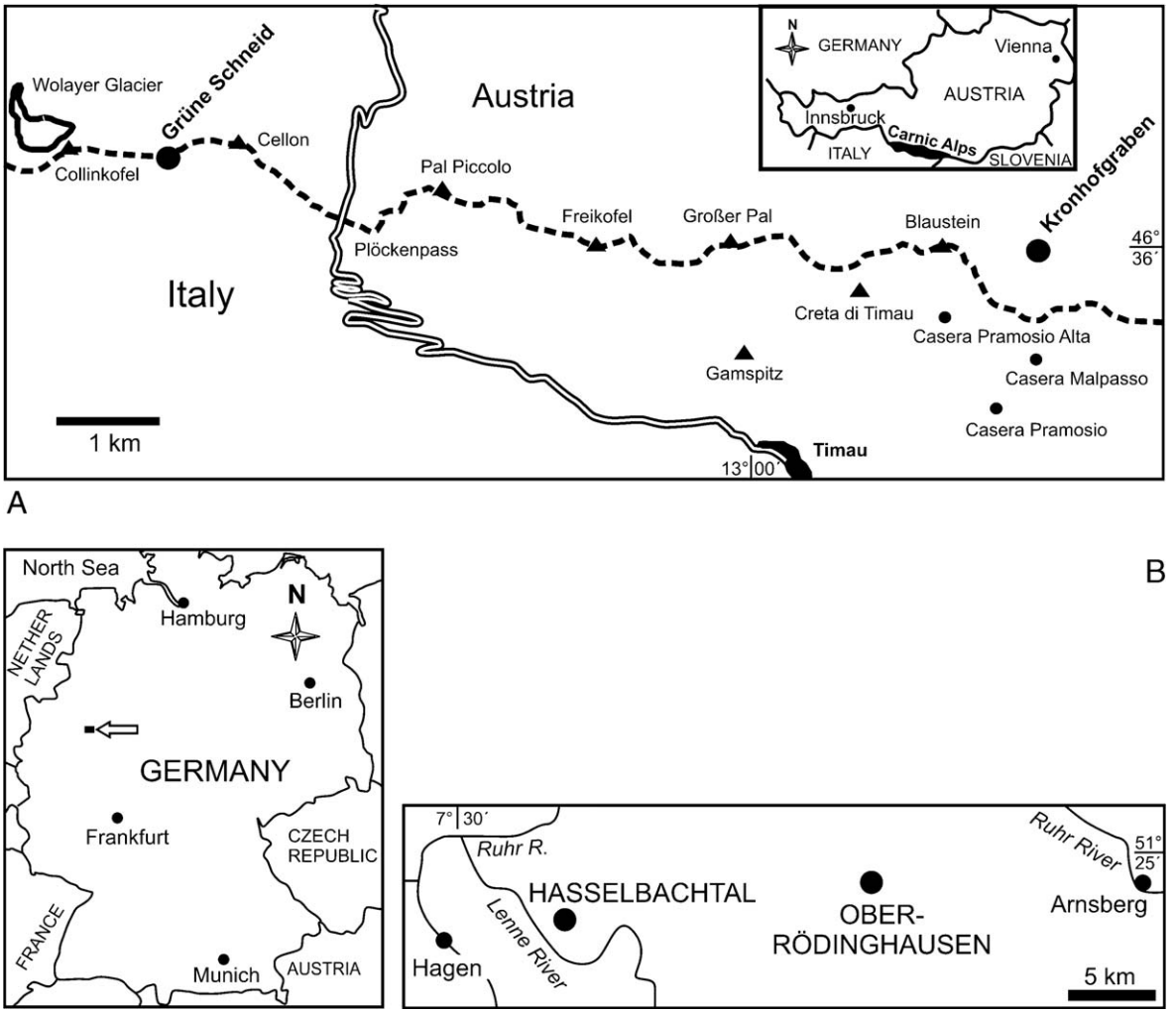

Fig. 2. Locality maps. (A) Carnic Alps, Austria and Italy; (B) Rhenish Massif, Germany.

geochemical excursions were found (Schönlaub et al., 1992, 1994). Due to the rather continuous sedimentation and high abundance of different faunal groups across the boundary interval, the Grüne Schneid section (Fig. 3) was proposed as a D/C boundary GSSP (Schönlaub et al., 1992), but the absence of siphonodellids at the boundary transition did not fulfil the criteria required, as the boundary is defined by the first occurrence of *S. sulcata* within the evolutionary lineage *Siphonodella praesulcata–S. sulcata*. The succession investigated comprises an interval between the Lower *praesulcata* and Lower *duplicata* zones, in accordance with previous results of conodont and ammonoid biostratigraphy (Schönlaub et al., 1988, 1992; Korn, 1992). The D/C boundary interval (Bed 6) was sampled on a cm-scale (Fig. 3). Bed 6b1 can be regarded as an equivalent of the Rhenish Hangenberg Black Shale, time-equivalent with the main extinction phase of the Hangenberg Event (Middle *praesulcata* Zone). This is indicated by the impoverished conodont fauna, the disappearance of other microfauna and ammonoids (Korn, 1992) at its base, and by a major faunal change from a pre-event bispathodid–branmehlid–palmatolepid biofacies to a post-event protognathodid–polygnathid biofacies (Fig. 3). The main regressive interval of the Hangenberg Event is not preserved at Grüne Schneid, but a rich faunal assemblage with abundant *P. kockeli* characterizes the Upper *praesulcata* Zone in Bed 6b2–6b3. Because of the absence of siphonodellids at the D/C boundary transition, a revised conodont zonation presented here is based on the protognathodid fauna, following Alberti et al. (1974), and Ziegler and Sandberg (1984). According to our results, the D/C boundary is drawn between Beds 6b3 and 6c, based on the first occurrence of *P. kuehni* in Bed 6c.

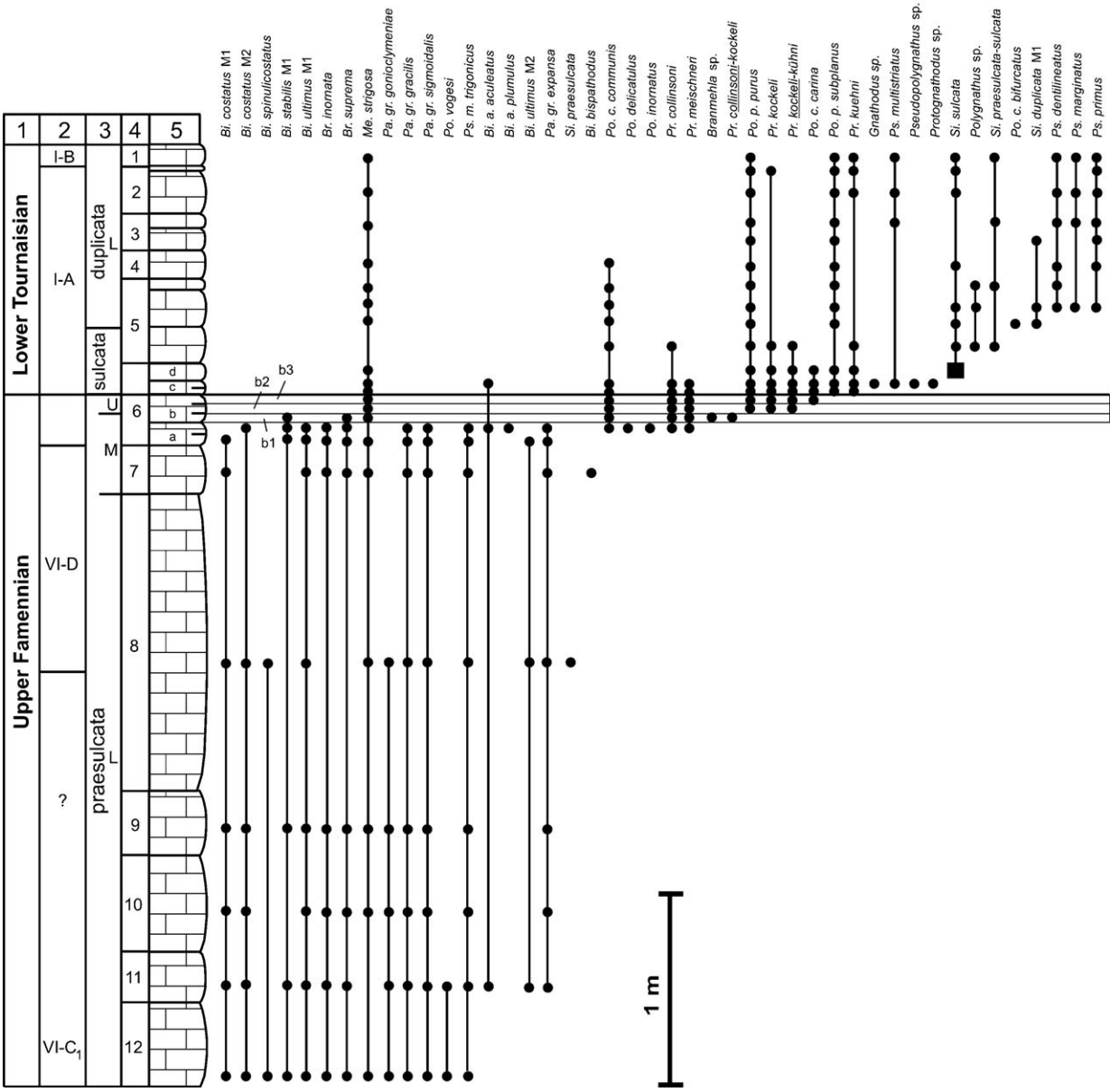

Fig. 3. Conodont biostratigraphy of D/C boundary section at Grüne Schneid (Carnic Alps, Austria). 1, Chronostratigraphy; 2, ammonoid zonal keys; 3, conodont zonation; 4, bed numbers; 5, lithostratigraphy. Ammonoid zonation from Korn (1992). Box = record of Schönlaub et al. (1992).

This contrasts previous studies (Schönlaub et al., 1988, 1992, 1994), which placed the boundary in Bed 6d, due to the first occurrence of *S. sulcata*.

The interval between the Lower *praesulcata* and *sandbergi* zones at Kronhofgraben (Fig. 4) was investigated previously (Schönlaub et al., 1992, 1994). *S. praesulcata*, the index species of the Lower *praesulcata* Zone, does not occur below Bed −1. In contrast to the records of Schönlaub et al. (1988), typical morphotypes of *P. gracilis gonioclymeniae* have not been recognized so that the base of the Middle *praesulcata* Zone, which is defined by the disappearance of *P. gracilis gonioclymeniae*, cannot be precisely determined. As discussed repeatedly (Over, 1992; Kürschner et al., 1993; Perri and Spalletta, 2000), its poor definition does not allow high-resolution correlation, and the zone is perhaps better abandoned. The absence of the zonal marker species is probably related to the deep depositional environment at Kronhofgraben, which is also confirmed by the scarcity of macrofauna in the micrites.

The cephalopod limestone beds at Kronhofgraben are interrupted by a 25 to 50 cm thick, unfossiliferous black

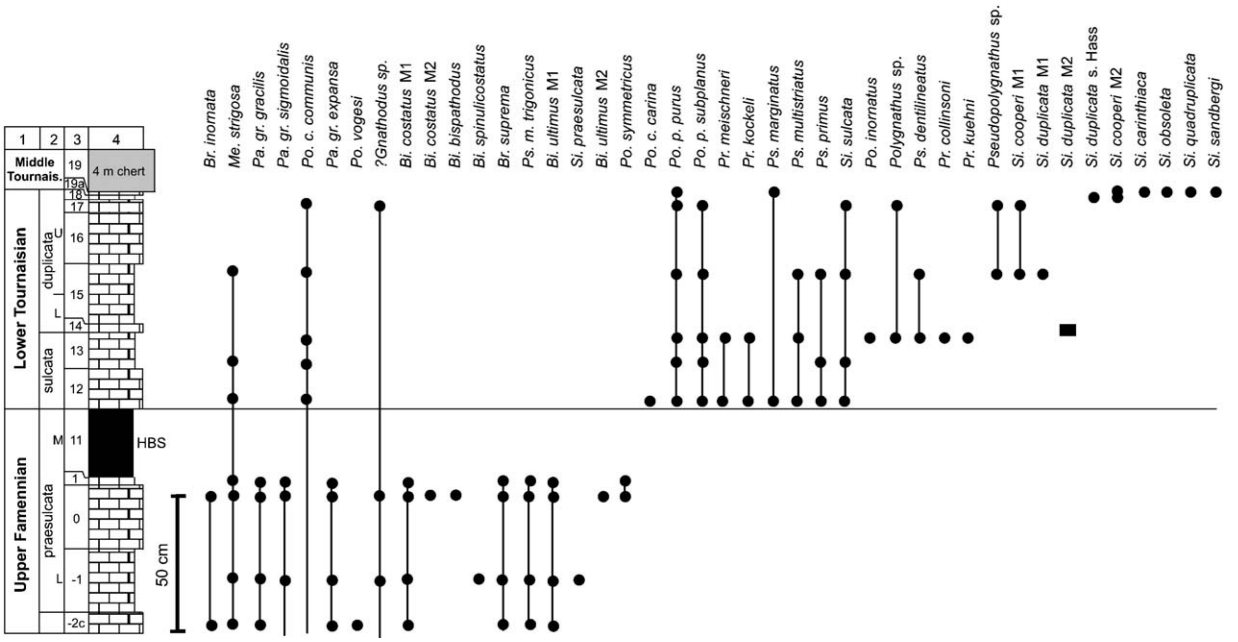

Fig. 4. Conodont biostratigraphy of D/C boundary section at Kronhofgraben (Carnic Alps, Austria). See Fig. 3 for explanation of keys to stratigraphical column. Box = record of Schönlaub et al. (1992); HBS = Hangenberg Black Shale.

shale horizon (Fig. 4, Bed 11), which has been considered as an equivalent of the Hangenberg Black Shale of Germany (Schönlaub et al., 1992). The Upper *praesulcata* Zone and the basal part of the *sulcata* Zone are not recorded due to the absence of the Lower and Upper *Protognathodus* conodont assemblages. A typical Carboniferous fauna with *S. sulcata* appears in Bed 12. The first *S. duplicata* Morphotype 1 occurs in Bed 14 (record of Schönlaub et al., 1992), and the top of Bed 15 contains morphotype 1 of *S. cooperi*, which defines the Upper *duplicata* Zone. The *sandbergi* Zone begins at the base of Bed 19a, in which *S. sandbergi* occurs together with *S. quadruplicata*, a marker fossil of the upper part of the *sandbergi* Zone (Sandberg et al., 1978). The complete *sandbergi* Zone is thus preserved within a highly condensed, 2 cm thick bed. This suggests that Bed 19, an overlying radiolarian-bearing chert horizon (Hahn and Kratz, 1992), is a time-equivalent of the Lower Alum Shale, which reflects a major sea-level rise at the base of the Middle Tournaisian (Becker, 1993; Becker and Weyer, 2004).

2.2. Rhenish Massif

Numerous studies on miospores, ammonoids, conodonts, the sedimentology and Sr-isotope stratigraphy (e.g., Becker, 1988, 1996; Kürschner et al., 1993; Higgs and Streel, 1994; Luppold et al., 1994; Korn and Weyer, 2003) addressed the D/C boundary auxiliary stratotype section (Becker and Paproth, 1993) at Hasselbachtal. The section (Fig. 5) became important due to the abundance of miospores, enabling the correlation between terrestrial and marine biostratigraphical records (Higgs and Streel, 1984). Intercalated meta-bentonite horizons allowed to derive numerical ages for the D/C boundary (360.2 ± 0.7 Ma; Trapp et al., 2004).

Conodonts indicate levels from the Upper *expansa* to the *sandbergi* Zone (Becker et al., 1984; Korn and Weyer, 2003). The micritic and nodular Wocklum Limestone contains a rich and diverse ammonoid fauna in association with a restricted benthic fauna that is typical for relative deep pelagic settings (the rhynchonellid *Novaplatirostrum*, small orthids, blind phacopids, small-sized solitary Rugosa, small heterocorals, cladochonid-type tabulate corals). At the top of the Wocklum Limestone (Bed 114N), limestone nodules become bioclastic and yielded oculated phacopids and proetids (Becker, 1996), which suggests a shallowing of the environments at the top of the *Epiwocklumeria applanata* Subzone (Upper Devonian VI-D2). The Hangenberg Black Shale (Bed 115) rests with sharp contact on the grey-green marly shales and nodules of Bed 114N and contains large weathered pyrite nodules right at the base and in the lower few centimetres. The lack of any bioturbation or endobenthos and the high pyrite content indicate a sudden change to anoxic oceanic facies. Somewhat higher there are mass occurrences of the bivalve *Guerichia*, associated with the last surviving

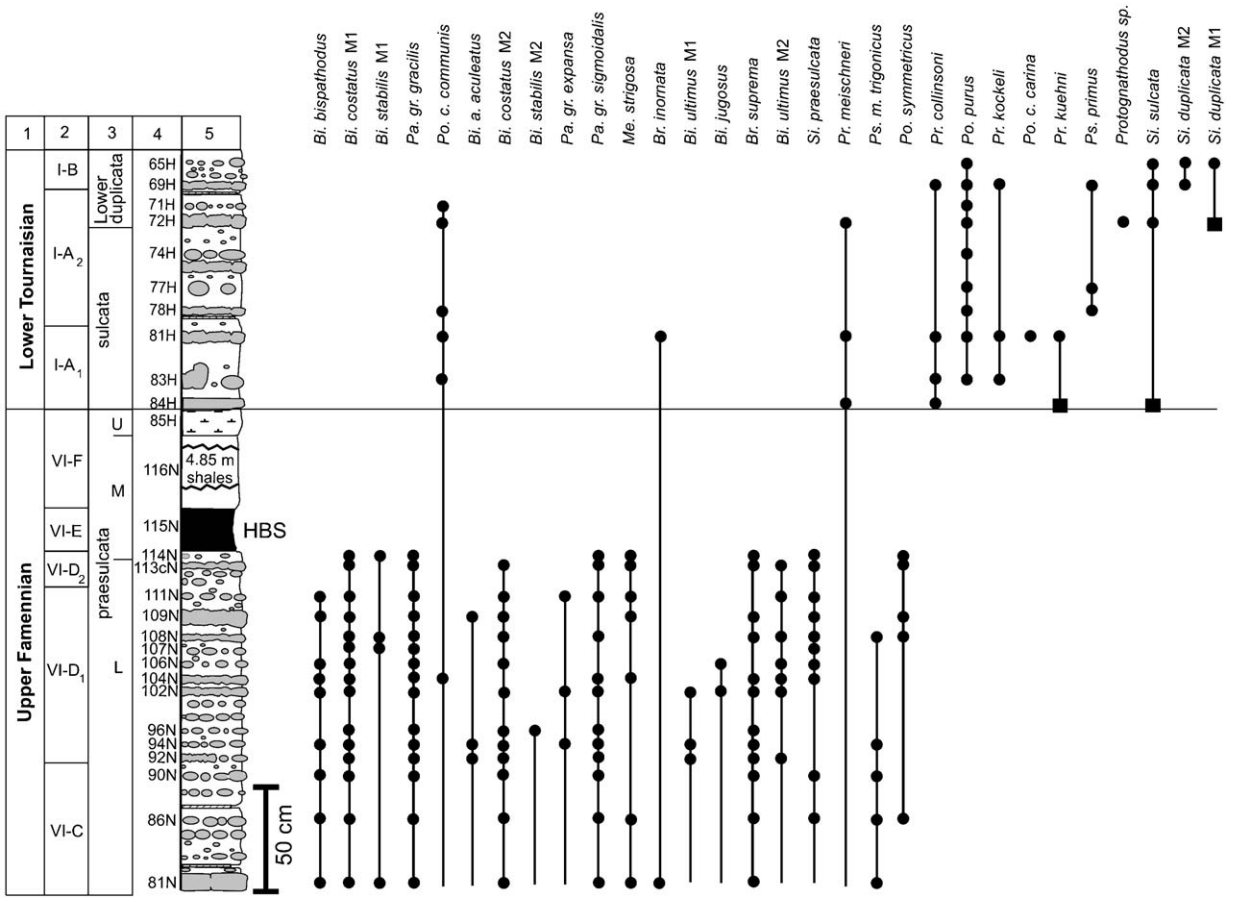

Fig. 5. Conodont biostratigraphy of D/C boundary section at Hasselbachtal (Rhenish Massif, Germany); ammonoid zonation based on Becker (1996), and Korn and Weyer (2003). See Fig. 3 for explanation of keys to stratigraphical column. Boxes=records of Becker et al. (1984).

clymenids. *Guerichia* is typical for the basinal Cypridinenschiefer facies of the Rhenish Massif, which was deposited basinwards from pelagic seamounts and carbonate ramps. At Hasselbachtal, the Hangenberg Black Shale is overlain by the green coloured, silty Hangenberg Shale (Bed 116N), while the Hangenberg Sandstone is locally replaced by fine-grained siliciclastics that cannot be separated from the Hangenberg Shale, due to a distal depositional environment.

Bed 116N is overlain by dark-grey marlstones (Bed 85H) with pyritic goniatites, bivalves, gastropods, and miospores, reflecting a rise in sea level and decreasing seafloor oxygenation in the Upper *praesulcata* Zone (Lower Stockum level). A shallowing just at the D/C boundary resulted in the deposition of crinoidal limestone (Bed 84H base) and a thin turbiditic limestone (Bed 84H top). The first *S. sulcata* occurs together with *P. kuehni* within Bed 84H, marking the base of the Carboniferous (Becker et al., 1984) at the base of the turbidite. Above, basal Tournaisian limestone deposits (Beds 83H to 81H) with the Upper *Protognathodus* fauna, lacking siphonodellids, but with some brachiopods, characterize the Upper Stockum level. Based on the entry of the ammonoid *Gattendorfia*, the Hangenberg Limestone commences with Bed 80H, immediately followed by the zircon-bearing bentonite Bed 79H. The Hangenberg Limestone looses macrofauna upsection, which has been interpreted as evidence for gradual deepening (Bless et al., 1993).

Due to the absence of *S. duplicata* Morphotype 1 in new samples from the Hangenberg Limestone, the base of the Lower *duplicata* Zone was fixed according to previous results (Kürschner et al., 1993) at the base of Bed 72H. The index fossil for the Upper *duplicata* Zone, *S. cooperi* Morphotype 1, is recorded in Bed 63H. Thus, the new conodont zonation presented here suggests a revised position of the Lower/Upper *duplicata* boundary, when compared to the records of Korn and Weyer (2003), who placed this boundary at the base of Bed 55H. In contrast to the cyclostratigraphic correlation of Korn and Weyer (2003), the base of the *sandbergi* Zone

is now fixed in Bed 49H, as indicated by the first occurrence of *S. obsoleta*.

3. Geochemical methods

Samples for $\delta^{13}C_{carb}$ analyses were drilled from polished slabs of micritic limestones, and transferred to an automated carbonate reaction device (Gas Bench II) connected to a ThermoFinnigan Delta S mass spectrometer. For the analysis of $\delta^{13}C_{org}$, HCl insoluble residues of samples were combusted offline, and the evolved CO_2 gas was submitted to mass spectrometric analysis after vacuum distillation. Total organic carbon (TOC) was determined coulometrically. The $\delta^{18}O_{phosph}$ values of conodont apatite were obtained by high-temperature reduction of Ag_3PO_4, which was prepared chemically after dissolving ~1 mg of conodont francolite in nitric acid (Wenzel et al., 2000). Three splits of the Ag_3PO_4 obtained from each sample passed the high-temperature reduction-mass-spectrometric analysis procedure, and 1 S.D. of the mean value of these analyses was better than 0.2‰ for most samples (Tables 1–4). Conodont samples consisted predominantly of monogeneric collections of *Palmatolepis*, *Protognathodus*, *Siphonodella*, and *Polygnathus*. To test for biological effects on the isotopic composition of conodont apatite, different genera were analyzed from several stratigraphical levels. These subsets differed by less than 0.8‰ $\delta^{18}O_{phosph}$ (Table 5). Isotopic compositions are reported relative to V-PDB ($\delta^{13}C$) and V-SMOW ($\delta^{18}O_{phosph}$), with an average analytical precision of ±0.1‰ $\delta^{13}C$ and 0.2‰ $\delta^{18}O_{phosph}$ (1 S.D.), derived from replicate analyses of NBS 19 ($\delta^{13}C_{carb}$), USGS 24 ($\delta^{13}C_{org}$), and NBS 120c ($\delta^{18}O_{phosph}$).

Table 1
Geochemical data from section at Grüne Schneid (Austria)

Bed no.	$\delta^{13}C_{carb}$ (‰ V-PDB)	$\delta^{13}C_{org}$ (‰ V-PDB)	TOC (%)	$\delta^{18}O_{phosph}$ (‰ V-SMOW)	1 S.D.	Genus[a]
2		−27.58	0.05			
2 top	2.63			18.98	0.10	Po
2b	2.63					
3b	2.52					
3a	2.72			18.75	0.07	Po
4	2.89	−28.13	0.15	18.58	0.20	Po
5c	2.64					
5b top	2.65					
5b	2.63	−28.77	0.03			
5a	2.75	−27.11	0.02	18.94	0.06	Po
6d		−30.30	0.10	18.86	0.20	Po
6d3	3.00					
6d2	2.92					
6d1	2.93					
6c		−27.04	0.06			
6c3	3.03					
6c2	2.97			19.12	0.12	Po
6c1	3.06	−26.02	0.06	19.16	0.06	Po
6b3	3.37			18.56	0.20	Po, Pr
6b3	3.42			18.81	0.20	Po, Pr
6b3	3.48					
6b3	3.63					
6b3	3.02					
6b2-3		−23.77	0.11			
6b2	3.52			19.39	0.06	Pr
6b2	3.43			19.47	0.35	Po, Pr
6b2	3.54					
6b2	3.68					
6b2	3.26					
6b2	3.55					
6b1	3.03	−24.10	0.11	18.63	0.20	Po, Pr
6b1	3.52					
6b1	3.50					
6b1	2.90					
6a		−26.84	0.08			
6a top	2.90					
6a top	2.70					
6a base	3.30			18.91	0.14	Pa
6a base	3.20					
7	2.81	−27.53	0.07	19.10	0.02	Pa
8	2.83			19.39	0.25	Pa
8 top		−28.00	0.12			
8 mid		−26.38	0.14			

[a] Pa=*Palmatolepis*, Po=*Polygnathus*, Pr=*Protognathodus*.

Table 2
Geochemical data from section at Kronhofgraben (Austria)

Bed no.	$\delta^{13}C_{carb}$ (‰ V-PDB)	$\delta^{13}C_{org}$ (‰ V-PDB)	TOC (%)	$\delta^{18}O_{phosph}$ (‰ V-SMOW)	1 S.D.	Genus[a]
19a	0.54			18.83	0.06	Si
18	0.73					
17	0.84					
16 top	1.74					
15 top	1.73					
15 base	1.60					
14	1.63					
13 top	2.16	−27.63	0.21	18.85	0.07	Po
13 base	1.79	−28.02	0.12			
12 top	1.91	−25.90	0.11			
12 base	1.92	−26.41	0.05	18.43	0.39	Po
11		−25.63	1.31			
1 top	2.30			19.25	0.07	Pa
1	2.25	−27.84	0.55			
0	2.19	−27.37	0.17	19.20	0.08	Pa
−1	2.55	−27.93	0.13			
−2c	2.54	−27.45	0.15			
−3b		−27.38	0.11			
−4				18.00	0.20	Pa

[a] Pa=*Palmatolepis*, Po=*Polygnathus*, Si=*Siphonodella*.

4. Results

From the base of the *praesulcata* Zone to the top of the *duplicata* Zone $\delta^{13}C_{carb}$ decreases in all studied

Table 3
Geochemical data from section at Hasselbachtal (Germany)

Bed no.	$\delta^{13}C_{carb}$ (‰ V-PDB)	$\delta^{13}C_{org}$ (‰ V-PDB)	TOC (%)	$\delta^{18}O_{phosph}$ (‰ V-SMOW)	1 S.D.	Genus[a]
69H/2	0.68					
71H	1.09					
72H	0.52					
74H	0.73					
76H/2	0.84					
77H	0.89	−26.84	0.06			
78H		−26.14	0.06			
80H		−26.85	0.06			
81H	0.40	−26.16	0.77	18.52	0.13	Po
82H		−26.19	0.09			
83H	0.58	−26.59	0.10			
84H top		−26.16	0.16			
85H top		−22.28	0.41			
116N top		−23.13	0.23			
116N3T		−22.64	0.56			
116 N3T		−22.55	0.56			
116N1T		−22.43	1.14			
115N mid		−21.70	0.88			
115N base		−24.75	2.10			
115N base		−24.76	2.10			
114N		−23.15	0.10			
113cN	1.35	−25.02	0.10	18.37	0.25	Pa
111N	1.47	−25.09	0.11			
109N	0.31	−24.29	0.90			
108bN	1.45					
107bN	1.46					
106N	1.51					
104N	1.70					
102N	1.33	−25.00	0.08			
96N	1.24					
94N	1.33					
92N	0.90					
90bN	1.43					
89N		−24.77	0.07			
86N	1.09	−25.63	0.04			
84N	1.41	−25.60	0.10			
81N	1.38					
8S				18.59	0.04	Pa

[a] Pa=*Palmatolepis*, Po=*Polygnathus*.

sections (Figs. 6 and 7). The $\delta^{13}C_{carb}$ values are generally higher in the micrites of the Carnic Alps when compared to those from Hasselbachtal (Rhenish Massif). In samples from a 10 cm thick, condensed succession of wacke- to mudstones at Grüne Schneid, $\delta^{13}C_{carb}$ increases to +3.7‰ (Fig. 6). This excursion begins in poorly fossiliferous time-equivalents of the Hangenberg Black Shale (Bed 6b1), and high values are also recorded from the Upper *praesulcata* Zone (Bed 6b2/3). This excursion remained unnoticed in previous studies of the section (Schönlaub et al., 1992, 1994), probably due to a much coarser sampling grid. No data are available from the black shales and sandstones of the lower to middle event interval from Hasselbachtal and Kronhofgraben (Fig. 6).

The $\delta^{13}C_{org}$ values (Fig. 7) from the Hasselbachtal section (−22‰ to −27‰) are generally higher than those from Grüne Schneid and Kronhofgraben (−24‰ to −30‰). A distinct excursion of +4‰ $\delta^{13}C_{org}$ was found in the Middle (Hangenberg Black Shale and equivalents) and Upper *praesulcata* Zone at Grüne Schneid and Hasselbachtal, while this excursion amounts to +2‰ $\delta^{13}C_{org}$ at Kronhofgraben, where the event interval is covered by a single sample (Fig. 6). At Grüne Schneid, the excursion parallels the less pronounced excursion in $\delta^{13}C_{carb}$ (Fig. 6). The TOC content in all sections is related to lithology and varies from ~0.1% in limestones to ~2% in shales.

Highest $\delta^{18}O_{phosph}$ values of c. 19.3‰ are recorded in conodonts from the top of the Lower *praesulcata* Zone at Kronhofgraben and Grüne Schneid, and at the base of the Upper *praesulcata* Zone at Grüne Schneid (Fig. 7). There is a decrease to 18.5‰ $\delta^{18}O_{phosph}$ in the Middle *praesulcata* Zone (Hangenberg Black Shale equivalents) at Grüne Schneid. While values are similar in sections from the Carnic Alps and the Rhenish Massif (Hasselbachtal, Oberrödinghausen) in both the Upper *expansa* Zone and in the Early Carboniferous, the $\delta^{18}O_{phosph}$ values in samples from the Carnic Alps are by ~1‰ higher in the upper part of the Lower *praesulcata* Zone. Grüne Schneid is the single section that provided $\delta^{13}C_{carb}$, $\delta^{13}C_{org}$, and $\delta^{18}O_{phosph}$ data from the same beds of the event interval. Variations in $\delta^{18}O_{phosph}$ are less than 1‰ and thus not significantly larger than in the over- and underlying levels of the sections studied.

5. Discussion

The overall trend of decreasing $\delta^{13}C_{carb}$ values from the Upper *expansa* to the *sandbergi* Zone is in accordance with low values in the subsequent lower

Table 4
Geochemical data from section at Oberrödinghausen (Germany)

Bed no.	Conodont zone	$\delta^{18}O_{phosph}$ (‰ V-SMOW)	1 S.D.	Genus[a]
3.1b	*duplicata*	18.47	0.23	Po
3b	*duplicata*	18.58	0.13	Si
6a	*sulcata*	18.42	0.26	Po
1a	*praesulcata*	18.45	0.08	Pa
3a	*praesulcata*	18.20	0.07	Pa
5	*praesulcata*	18.87	0.02	Pa
10a	*praesulcata*	18.38	0.16	Pa

Bed numbers after Schindewolf (1937; Wocklum Limestone, Beds 10a–1a) and Vöhringer (1960; Hangenberg Limestone, Beds 6a–3.1b).
[a] Pa=*Palmatolepis*, Po=*Polygnathus*, Si=*Siphonodella*.

Table 5
$\delta^{18}O_{phosph}$ (‰ V-SMOW) of samples of various conodont genera

Sample no.	Conodont genera				
	Siphonodella	*Palmatolepis*	*Polygnathus*	*Protognathodus*	*Polygn./Protogn.*
GS 6c			19.48±0.14	18.92±0.24	
GS 6b			18.71±0.20	19.39±0.06	18.60±0.33
GS 12		18.74±0.20	18.59±0.11		
Oröha 3b	18.58±0.13		18.47±0.23		

part of the mid-Tournaisian (Saltzman et al., 2000). Generally higher values in micrites from the Carnic Alps when compared to the Rhenish Massif are difficult to evaluate as the origin of micrite in pelagic Palaeozoic limestone is mostly unknown. Litho- and biofacies of the studied sections indicate roughly similar water depth well below the photic zone, and above the implosion depth for goniatites (i.e. 100–250 m).

Our biostratigraphic correlation, utilizing the finest time resolution available, indicates that the excursion to high $\delta^{13}C_{carb}$ and $\delta^{13}C_{org}$ values in the Middle *praesulcata* Zone of the Grüne Schneid section is time-equivalent to the deposition of black shales elsewhere (Hangenberg Black Shale of the Rhenish Massif, equivalents of Thuringia, the Carnic Alps, southern France, Morocco, Iran, Lower Exshaw and Lower Bakken Shale of Canada, Conchostracan Shale of U.S. Interior, basal Bedford Shale of Ohio, Changshun Shale of South China, etc.), corresponding to a sea-level highstand just above the main extinction phase of the Hangenberg Event (Becker, 1993; Wagner, 2001). High $\delta^{13}C_{org}$ values are also found in the Upper *praesulcata* Zone of all studied sections (Fig. 6), and even in the lower part of the *sulcata* Zone at Kronhofgraben, and thus persisted much longer than the episode of globally widespread black shale deposition. As outlined above, a significant positive excursion reported from brachiopods of the Louisiana Limestone (Brand et al., 2004) falls in the Upper *praesulcata* Zone and coincides with high $\delta^{13}C_{carb}$ and $\delta^{13}C_{org}$ values of the same level at Grüne Schneid, but is not correlative to the Hangenberg Black Shale.

The Grüne Schneid section is exceptional, as it recorded almost continuous carbonate deposition across the D/C boundary during an episode of a global "carbonate crisis" characterized elsewhere by black shales and siliciclastics. The event interval (base of Middle *praesulcata* to Middle *sulcata* Zone) comprises less than 1 m and the main regressive phase, equivalent to the Hangenberg Sandstone of the Rhenish Massif, is not preserved. This hiatus does not correspond to a prominent non-depositional surface but occurs over a 3 cm thick level of micritic limestones with dissolution seams. Condensation of the event beds and sediment mixing by bioturbation must be invoked to have disturbed the preservation of the complete geochemical record. The Upper *praesulcata* Zone is c. 10 cm thick at Grüne Schneid and Hasselbachtal and the excursion of both $\delta^{13}C_{carb}$ and $\delta^{13}C_{org}$ values is much smaller than that reported for the several metres thick, time-equivalent Louisiana Limestone, where $\delta^{13}C_{carb}$ values of up to +7‰ have been recorded in brachiopod calcite (Brand et al., 2004). This suggests that the sections at Hasselbachtal and Grüne Schneid may be incomplete in the Upper *praesulcata* Zone. However, in the Middle *praesulcata* Zone, the amplitude of the $\delta^{13}C_{org}$ excursion is similar in the condensed pelagic limestones at Grüne Schneid and the much thicker shales and black shales at Hasselbachtal (Fig. 6). Also, the excursion in brachiopod $\delta^{13}C_{carb}$ values at La Serre (GSSP; Brand et al., 2004) is similar in magnitude when compared to micrites from Grüne Schneid, so that an amalgamation of the excursion at Grüne Schneid by bioturbation and condensation is unlikely for the Middle *praesulcata* Zone. Therefore, the different amplitudes of the $\delta^{13}C_{org}$ (+4‰) and $\delta^{13}C_{carb}$ (+1.2‰) excursions need to be explained. A significant contribution of terrestrial organic matter, with mean values of −25‰ to −24‰ (Strauss and Peters-Kottig, 2003), can be excluded because the organic matter of the Hangenberg Black Shale at Hasselbachtal is mostly amorphous, and contains significantly less spores than the under- and overlying green shales (Higgs and Streel, 1994; J. Richardson, written com.). A marine origin of C_{org} and increased marine primary productivity is confirmed by mass occurrences of specific pelagic consumers such as the bivalve *Guerichia* in the Hangenberg Black Shale. Bursts of single photosynthetic acritarch species in the contemporaneous black Exshaw Shale of the Canadian Rocky Mountains have been noted by Audretsch (1967). At Grüne Schneid, the pure pelagic limestones that contain the excursion are C_{org}-poor and almost free of siliciclastics.

Differences in the amplitude of $\delta^{13}C_{carb}$ and $\delta^{13}C_{org}$ excursions have been reported previously (e.g., Hayes et al., 1989; Kuypers et al., 1998) and explained by a

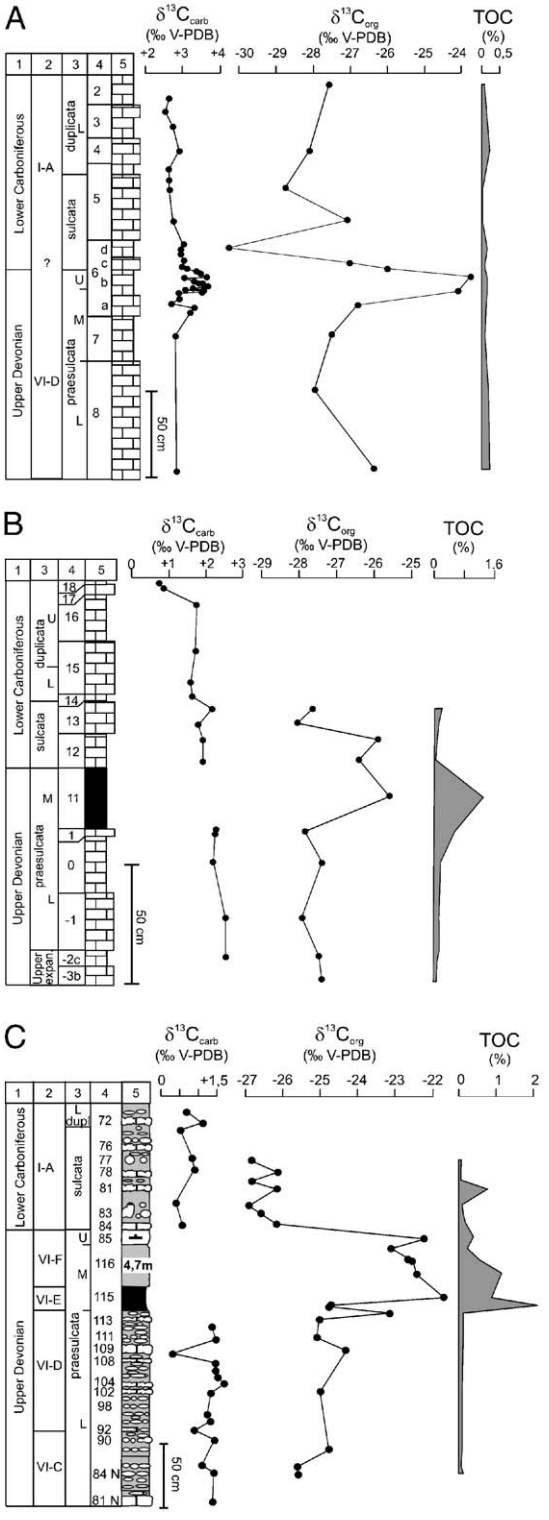

Fig. 6. Stratigraphy and geochemical data of D/C boundary section at (A) Grüne Schneid, (B) Kronhofgraben (Carnic Alps, Austria), and (C) Hasselbachtal (Rhenish Massif, Germany). See Fig. 3 for explanation of keys to stratigraphical column.

change in the carbon isotope fractionation during photosynthesis as a result of a changing pCO_2 of sea-surface waters (Hayes et al., 1999). Lowering of pCO_2 is expected to result in a decrease in the carbon-isotope fractionation during photosynthesis, and could explain the larger amplitude in $\delta^{13}C_{org}$. A decrease in pCO_2 of sea-surface waters, and thus a lower photosynthetic carbon isotope fractionation during the event interval appears likely due to the enhanced burial of organic carbon as evidenced by the globally widespread black shales, and is mirrored in the $\delta^{13}C_{carb}$ values. On the short time scales discussed here, the globally reduced formation of carbonates during the event interval has also potentially reduced the pCO_2 of seawater (Ridgwell et al., 2003). As carbon isotope fractionation during $CaCO_3$ precipitation is rather small, the contribution of globally diminished carbonate formation to the reduction of atmospheric pCO_2 is not seen in the $\delta^{13}C_{carb}$ values, which indicate only moderately enhanced C_{org} burial when compared to other episodes of global black shale deposition. Nevertheless, increased burial of organic matter during the event interval is well documented, and must have resulted in the drawdown of atmospheric CO_2 that may have contributed to climatic cooling, a glacial advance in Gondwana (Streel et al., 2000), and a major glacial-eustatic sea-level fall as reflected in the Hangenberg Sandstone and its global equivalents.

Previous studies on Palaeozoic conodonts suggested that the oxygen isotope composition of conodont apatite is a reliable proxy for reconstructing the $\delta^{18}O$ composition and palaeotemperature of sea-surface water (Joachimski and Buggisch, 2002; Joachimski et al., 2004). Conodont apatite is composed of well-crystallized fluorapatite and structurally comparable to tooth enamel which has a high potential to preserve its primordial isotope composition (Kolodny et al., 1983; Lécuyer et al., 1999). Analysis of Silurian and Late Devonian conodont apatite showed that oxygen isotope ratios are significantly higher than the values of contemporaneous calcitic brachiopod shells (Wenzel et al., 2000; Joachimski et al., 2004). Most important, the $\delta^{18}O$ values of conodonts give realistic temperatures whereas the $\delta^{18}O$ values of brachiopod shells translate into unrealistically warm temperatures. Since neither diagenetic overprinting nor non-equilibrium fractionation can account for the higher $\delta^{18}O$ values of conodont apatite in comparison to brachiopod calcite, Wenzel et al. (2000) and Joachimski et al. (2004) argued that conodont apatite $\delta^{18}O$ values may represent a more reliable recorder of Palaeozoic palaeotemperature than the $\delta^{18}O$ values of brachiopod calcite.

Disregarding changes in the $\delta^{18}O$ of seawater, the following chronology of climate change is seen in the $\delta^{18}O_{phosph}$ data: high temperatures and the absence of a

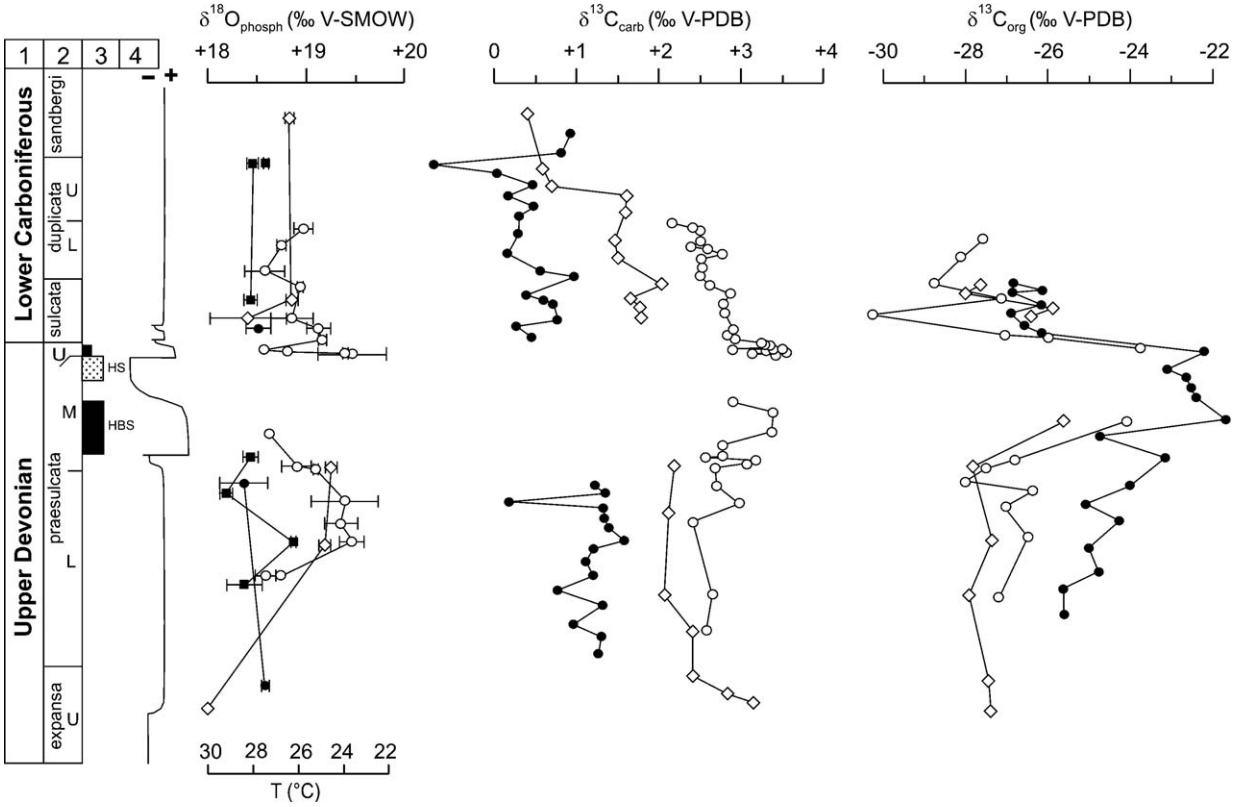

Fig. 7. Correlation of geochemical data from sections in the Carnic Alps (open circles = Grüne Schneid, diamonds = Kronhofgraben) and the Rhenish Massif (black dots = Hasselbachtal, black boxes = Oberrödinghausen). Relative thickness of conodont zones derived from assumption that correlated ammonoid genozones (Fig. 1) represent roughly equal time units (Becker, 1996). 1, Chronostratigraphy; 2, conodont biozones; 3, distinctive lithofacies of the Hangenberg Event interval, HBS = Hangenberg Black Shale, HS = Hangenberg Sandstone, locally overlain by black shales or organic-rich limestone. Palaeotemperatures calculated from $\delta^{18}O_{phosph}$ after Kolodny et al. (1983), assuming −1‰ $\delta^{18}O$ (V-SMOW) of Devonian seawater (Joachimski and Buggisch, 2002).

latitudinal thermal gradient are recorded in samples from the *expansa–praesulcata* transition. A decrease in sea-surface temperature in the Early *praesulcata* Zone was followed by an increase to higher temperatures that began in the late Early *praesulcata* Zone, and persisted during the deposition of the Hangenberg Black Shale, corresponding to the mass extinction phase of the event interval. The drop in temperature during the Early *praesulcata* Zone was apparently more significant at 20° southern latitude (~4 °C) than in equatorial settings (~2 °C), although these latitudinal differences are close to the analytical precision of the $\delta^{18}O_{phosph}$ values, and to the variations observed among different genera from one sample (Table 5). High temperatures during the formation of the Hangenberg Black Shale are in accordance with palynological evidence of a major change from arid to humid climate in South America and Greenland (Streel et al., 2000; Marshall et al., 2002), enabling the buildup of continental glaciers in high latitudes, and resulting in the major drop in sea-level recorded in the Hangenberg Sandstone and its equivalents. We have no $\delta^{18}O_{phosph}$ data from deposits which are time-equivalent to the Hangenberg Sandstone. At the La Serre stratotype, Brand et al. (2004) recorded the highest $\delta^{18}O$ values (up to +0.3‰) in Bed 82, but due to biostratigraphical uncertainty as discussed above, it is impossible to decide whether these brachiopods come from the top part of the Middle *praesulcata* Zone or from the Upper *praesulcata* Zone. The decrease in $\delta^{18}O_{phosph}$ of 1‰ in the Upper *praesulcata* Zone at Grüne Schneid indicates a temperature increase of ~4 °C after the main regressive phase, or a change in the $\delta^{18}O$ of seawater related to the melting of an ice sheet of similar volume than that of the last Quaternary glaciation. This is in accordance with the significant transgression recognized at this level (Fig. 7; Bless et al., 1993; Becker, 1996). Changes in $\delta^{18}O_{phosph}$ during the event interval are not larger than during the Early and Middle *praesulcata* Zone, but considering the

absence of data from the main regressive episode of the extinction event, our data most likely provide a minimum estimate of changes in $\delta^{18}O_{phosph}$ during the latest Devonian. The D/C boundary at Grüne Schneid is marked by an insignificant drop in temperature, and no latitudinal gradient in palaeotemperature is evident in the $\delta^{18}O_{phosph}$ values from the lowermost Carboniferous.

At least for the event interval, the $\delta^{18}O_{phosph}$ record certainly represents a combination of both ice volume and temperature effects, but their relative contributions to the observed variations are difficult to quantify. The observation that the latitudinal apparent temperature gradient increased during the cooler episode of the early *praesulcata* Zone may suggest that changes in the $\delta^{18}O$ of seawater were not the major control of $\delta^{18}O_{phosph}$ values before the event interval, and that these variations can be ascribed largely to changes in palaeotemperature.

6. Conclusions

The correlation of geochemical proxies by high resolution biostratigraphy indicates a complex pattern of environmental change around the D/C boundary that is remarkably similar to other mass extinction events of the Phanerozoic. An episode of low-latitude warming, beginning in the latest Early *praesulcata* Zone, was followed by the globally widespread deposition of black shales. Sea-surface temperatures during the deposition of the Hangenberg Black Shale were not exceptionally high when compared to those of the earliest *praesulcata* Zone and the earliest Carboniferous. High rates of C_{org} burial and drawdown of atmospheric CO_2 are evidenced by a positive carbon isotope excursion, with a larger amplitude in bulk organic matter when compared to carbonate carbon. This contributed to global cooling, as indicated by a short-lived glacial pulse in Gondwana, and a major glacial-eustatic drop in sea level, consistent with palynological evidence of cool and humid conditions (Streel et al., 2000). In the latest Devonian (Late *praesulcata* Zone) climate warming and the melting of ice sheets in Gondwana resulted in a rising sea level, with $\delta^{13}C$ values similar to those of the previous main extinction event.

The major extinction event at the D/C boundary has to be evaluated in terms of a complex pattern of climate change, resulting in glacial-eustatic sea-level change as well as oceanic shelf anoxia and related perturbations in the carbon cycle, which affected both the marine and the terrestrial biosphere. Although the ultimate cause for black shale deposition at the end of the Devonian is unknown, our data support the hypothesis that oceanic anoxia and increased C_{org} burial can trigger mass extinctions, glaciations and eustatic sea-level change.

Acknowledgments

The help of S. Pohler and M.W. Rasser during fieldwork is gratefully acknowledged. S. Breisig gave valuable advice for the preparation of conodont samples. Funding was provided by Deutsche Forschungsgemeinschaft (Grant Ste 670/4).

References

Alberti, H., Groos-Uffenorde, H., Streel, M., Uffenorde, H., Walliser, O.H., 1974. The stratigraphical significance of the *Protognathodus* fauna from Stockum (Devonian/Carboniferous boundary, Rhenish Schiefergebirge). Newsl. Stratigr. 3, 263–276.

Alekseev, A.A., Lebedev, O.A., Barskov, I.S., Barskova, M.I., Kononova, L.I., Chizhova, V.A., 1994. On the stratigraphic position of the Famennian and Tournaisian fossil vertebrate beds in Andreyevka, Tula Region, central Russia. Proc. Geol. Assoc. 105, 41–52.

Almond, J., Marshall, J., Evans, F., 2002. Latest Devonian and earliest Carboniferous glacial events in South Africa. 16th Internat. Sed. Congr., Abstracts, pp. 11–12.

Audretsch, A.P., 1967. A Middle Devonian microflora from the Great Slave Lake area, Northwest Territories, Canada. In: Oswald, D.H. (Ed.), International Symposium on the Devonian System II. Alberta Society of Petroleum Geologists, Calgary, Canada, pp. 837–847.

Bai, S., 1988. Devonian possible impact events. Progr. Geosci. China, Papers to 28th IGC, pp. 139–142.

Becker, R.T., 1988. Ammonoids from the Devonian–Carboniferous boundary in the Hasselbach Valley (northern Rhenish Slate Mountains). Cour. Forschungsinst. Senckenberg 100, 193–213.

Becker, R.T., 1993. Analysis of ammonoid palaeobiogeography in relation to the global Hangenberg (terminal Devonian) and Lower Alum Shale (Middle Tournaisian) events. Ann. Soc. Géol. Belg. 115, 459–473.

Becker, R.T., 1996. New faunal records and holostratigraphic correlation of the Hasselbachtal D/C-boundary auxiliary stratotype (Germany). Ann. Soc. Géol. Belg. 117, 19–45.

Becker, R.T., Paproth, E., 1993. Auxiliary stratotype sections for the Global Stratotype Section and Point (GSSP) for the Devonian-Carboniferous boundary: Hasselbachtal. Ann. Soc. Géol. Belg. 115, 703–706.

Becker, R.T., Weyer, D., 2004. *Bartzschiceras* n. gen. (Ammonoidea) from the Lower Tournaisian of southern France. Mitt. Geol.-Paläontol. Inst. Univ. Hamb. 88, 11–36.

Becker, R.T., Bless, M.J.M., Brauckmann, C., Friman, L., Higgs, K., Keupp, H., Korn, D., Langer, W., Paproth, E., Racheboeuf, P., Stoppel, D., Streel, M., Zakowa, H., 1984. Hasselbachtal, the section best displaying the Devonian-Carboniferous boundary beds in the Rhenish Massif (Rheinisches Schiefergebirge). Cour. Forschungsinst. Senckenberg 67, 23–28.

Bless, M.J.M., Becker, R.T., Higgs, K., Paproth, E., Streel, M., 1993. Eustatic cycles around the Devonian–Carboniferous boundary and the sedimentary and fossil record in Sauerland (Federal Republic of Germany). Ann. Soc. Géol. Belg. 115, 689–702.

Brand, U., Legrand-Blain, M., Streel, M., 2004. Biochemostratigraphy of the Devonian–Carboniferous boundary global stratotype section and point, Griotte Formation, La Serre, Montagne Noire, France. Palaeogeogr. Palaeoclimatol. Palaeoecol. 205, 337–357.

Caputo, M.V., 1985. Late Devonian glaciation in South America. Palaeogeogr. Palaeoclimatol. Palaeoecol. 148, 187–207.

Casier, J.-G., Lethiers, F., Préat, A., 2002. Ostracods and sedimentology of the Devonian–Carboniferous stratotype section (La

Serre, Montagne Noire, France). Bull. Inst. R. Sci. Nat. Belg. 72, 43–68.

Casier, J.-G., Mamet, B., Préat, A., Sandberg, C.A, 2004. Sedimentology, conodonts and ostracods of the Devonian–Carboniferous strata of the Anseremme railway bridge section, Dinant Basin, Belgium. Bull. Inst. R. Sci. Nat. Belg. 74, 45–68.

Casier, J.-G., Lebon, A., Mamet, B., Préat, A., 2005. Ostracods and lithofacies close to the Devonian–Carboniferous boundary in the Chanxhe and Rivage sections, northeastern part of the Dinant Basin, Belgium. Bull. Inst. R. Sci. Nat. Belg. 75, 95–126.

Chauffe, K.M., Nichols, P.A., 1995. Multielement conodont species from the Louisiana Limestone (Upper Devonian) of west-central Illinois and northeastern Missouri, U.S.A. Micropaleontology 41, 171–186.

Hahn, G., Kratz, R., 1992. Eine Trilobitenfauna des tiefen Wassers aus dem Unterkarbon der Karnischen Alpen-Vorläufige Mitteilung. Jb. Geol. B.-A. 134, 217–224.

Hayes, J.M., Popp, B.N., Takigiku, R., Johnson, M.W., 1989. An isotopic study of biogeochemical relationships between carbonates and organic carbon in the Greenhorn Formation. Geochim. Cosmochim. Acta 53, 2961–2972.

Hayes, J.M., Strauss, H., Kaufman, A.J., 1999. The abundance of ^{13}C in marine organic matter and isotopic fractionation in the global biogeochemical cycle of carbon during the past 800 Ma. Chem. Geol. 161, 103–125.

Higgs, K.T., Streel, M., 1994. Palynological age for the lower part of the Hangenberg Shales in Sauerland, Germany. Ann. Soc. Géol. Belg. 116, 243–247.

Holser, W., Magaritz, M., Ripperdan, R.L., 1996. Global isotopic events. In: Walliser, O.H. (Ed.), Global Events and Event Stratigraphy in the Phanerozoic. Lect. Notes Earth Sci., vol. 30, pp. 63–88.

House, M.R., 1985. Correlation of mid-Paleozoic ammonoid evolutionary events with global sedimentary perturbations. Nature 313, 17–22.

House, M.R., 2002. Strength, timing, setting and cause of mid-Palaeozoic extinctions. Palaeogeogr. Palaeoclimatol. Palaeoecol. 181, 5–25.

Isaacson, P.E., Hladil, J., Shen, J.W., Kalvoda, J., Grader, G., 1999. Late Devonian (Famennian) glaciation in South America and marine offlap on other continents. Abh. Geol. B.-A. 54, 239–257.

Joachimski, M.M., Buggisch, W., 2002. Conodont apatite $\delta^{18}O$ signatures indicate climatic cooling as a trigger of the Late Devonian mass extinction. Geology 30, 711–714.

Joachimski, M.M., van Geldern, R., Breisig, S., Day, J., Buggisch, W., 2004. Oxygen isotope evolution of biogenic calcite and apatite during the Middle and Late Devonian. Int. J. Earth Sci. 93, 542–553.

Kolodny, Y., Luz, B., Navon, O., 1983. Oxygen isotope variations in phosphate of biogenic apatites. I. Fish bone apatite—rechecking the rules of the game. Earth Planet. Sci. Lett. 64, 398–404.

Korn, D., 1992. Ammonoideen vom Devon/Karbon-Grenzprofil an der Grünen Schneid (Karnische Alpen, Österreich). Jb. Geol. B.-A. 135, 7–19.

Korn, D., Weyer, D., 2003. High resolution stratigraphy of the Devonian–Carboniferous transitional beds in the Rhenish Mountains. Mitt. Mus. Nat.kd. Berl., Geowiss. Reihe 6, 79–124.

Kürschner, W., Becker, R.T., Buhl, D., Veizer, J., 1993. Strontium isotopes in conodonts: Devonian–Carboniferous transition, the northern Rhenish Slate Mountains, Germany. In: Streel, M., Sevastopulo, G., Paproth, E. (Eds.), Devonian–Carboniferous boundary. Ann. Soc. Géol. Belgique, vol. 115, pp. 595–621.

Kuypers, M.M., Schouten, S., Sinninghe Damsté, J.S., 1998. The Cenomanian/Turonian oceanic anoxic event: response of the atmospheric CO_2 level. Mineral. Mag. 62A, 836–837.

Lécuyer, C., Grandjean, P., Sheppard, S.M.F., 1999. Oxygen isotope exchange between dissolved phosphate and water at temperatures <135 °C: inorganic versus biological fractionations. Geochim. Cosmochim. Acta 63, 855–862.

Luppold, F.W., Clausen, C.-D., Korn, D., Stoppel, D., 1994. Devon/Karbon-Grenzprofile im Bereich von Remscheid-Altenaer Sattel, Warsteiner Sattel, Briloner Sattel und Attendorn-Elsper Doppelmulde (Rheinisches Schiefergebirge). Geol. Paläontol. Westf. 29, 7–69.

Marshall, J.E.A., Astin, T.R., Evans, F., Almond, J., 2002. The palaeoclimatic significance of the Devonian–Carboniferous boundary. Geology of the Devonian System. Proceedings of the International Symposium, July 9–12, 2000. Syktyvkar, Komi Republic, pp. 23–25.

Matyja, H., Stempien-Salek, M., 1994. Devonian/Carboniferous boundary and the associated phenomena in western Pomerania (NW Poland). Ann. Soc. Géol. Belg. 116, 249–263.

Olempska, E., 1997. Changes in benthic ostracod assemblages across the Devonian–Carboniferous boundary in the Holy Cross Mountains, Poland. Acta Palaeontol. Pol. 42, 291–332.

Over, D.J., 1992. Conodonts and the Devonian–Carboniferous boundary in the Upper Woodford Shale, Arbuckle Mountains, south-central Oklahoma. J. Paleontol. 66, 293–311.

Paproth, E., 1986. An introduction to a field trip to the Late Devonian outcrops in the northern Rheinisches Schiefergebirge (Federal Republic of Germany). Ann. Soc. Géol. Belg. 109, 275–284.

Perri, M.C., Spalletta, C., 2000. Late Devonian–Early Carboniferous transgressions and regressions in the Carnic Alps (Italy). Rec. West. Aust. Mus., Suppl. 58, 305–319.

Ridgwell, A.J., Kennedy, M.J., Caldeira, K., 2003. Carbonate deposition, climate stability, and Neoproterozoic ice ages. Science 302, 859–862.

Saltzman, M.R., González, L.A., Lohmann, K.C., 2000. Earliest Carboniferous cooling step triggered by the Antler orogeny? Geology 28, 347–350.

Sandberg, C.A., Streel, M., Scott, R.A., 1972. Comparison between conodont zonation and spore assemblages at the Devonian–Carboniferous boundary in the western and central United States and in Europe. C. R. 7th Congr. Internat. Strat. Géol. Carb., vol. 1, pp. 179–203.

Sandberg, C.A., Ziegler, W., Leuteritz, K., Brill, S.M., 1978. Phylogeny, speciation, and zonation of *Siphonodella* (Conodonta, Upper Devonian and Lower Carboniferous). Newsl. Stratigr. 7, 102–120.

Sandberg, C.A., Poole, F.G., Johnson, J.G., 1988. Upper Devonian of western United States. In: McMillan, N.J., et al. (Ed.), Devonian of the World. Proceedings of the Canadian Society of Petrology and Geology International Symposium. Devonian System Memoir, vol. 14, pp. 183–220.

Schindewolf, O.H., 1937. Zur Stratigraphie und Paläontologie der Wocklumer Schichten (Oberdevon). Abh. Preuβ. Geol. L.-Anstalt, N. F. 178, 1–132.

Schönlaub, H.P., Feist, R., Korn, D., 1988. The Devonian–Carboniferous boundary at the section "Grüne Schneid" (Carnic Alps, Austria): a preliminary report. Cour. Forschungsinst. Senckenberg 100, 149–167.

Schönlaub, H.P., Attrep, M., Boeckelmann, K., Dreesen, R., Feist, R., Fenninger, A., Hahn, G., Klein, P., Korn, D., Kratz, R., Magaritz, M., Orth, C.J., Schramm, J.-M, 1992. The Devonian/Carboniferous boundary in the Carnic Alps (Austria)—a multidisciplinary approach. Jb. Geol. B.-A. 135, 57–98.

Schönlaub, H., Kreutzer, L., Joachimski, M.M., Buggisch, W., 1994. Sedimentology and geochemistry of boundary sections from the Northern Calcareous (K/T) and Carnic Alps (O/S, S/D, F/F, D/C,

P/T). In: Joachimski, M.M. (Ed.), Sedimentology and geochemistry of boundary sections from the northern Calcareous (K/T) and Carnic Alps (O/S, S/D, F/F, D/C, P/T), Austria—a field guide. Erlanger Geol. Abh., vol. 122, pp. 77–103.

Scott, A.J., 1961. Three new conodonts from the Louisiana Limestone (Upper Devonian) of Western Illinois. J. Paleontol. 35, 1222–1243.

Sepkoski Jr., J.J., 1996. Patterns of Phanerozoic extinction: a perspective from global data bases. In: Walliser, O.H. (Ed.), Global Events and Event Stratigraphy in the Phanerozoic. Springer, Berlin, pp. 35–51.

Strauss, H., Peters-Kottig, W., 2003. The Paleozoic to Mesozoic carbon cycle revisited: the carbon isotopic composition of terrestrial organic matter. Geochem. Geophys. Geosyst. 4, doi:10.1029/2003GC000555.

Streel, M., Caputo, M.V., Loboziak, S., Melo, J.H.G., 2000. Late Frasnian–Famennian climates based on palynomorph analyses and the question of the Late Devonian glaciations. Earth-Sci. Rev. 52, 121–173.

Trapp, E., Kaufmann, B., Mezger, K., Korn, D., Weyer, D., 2004. Numerical calibration of the Devonian–Carboniferous boundary: two new U–Pb ID-TIMS single-zircon ages from Hasselbachtal (Sauerland, Germany). Geology 32, 857–860.

Vöhringer, E., 1960. Die Goniatiten der unterkarbonischen Gattendorfia-Stufe im Hönnetal (Sauerland). Fortschr. Geol. Rheinl. Westfal. 3, 107–196.

Wagner, P., 2001. Palynology at the Devonian/Carboniferous Boundary: discussion of the sedimentological environment at sampled sections in Portugal, Ireland, U.S.A., and Canada. Zentralbl. Geol. Paläontol., Teil 1, 185–197.

Walliser, O.H., 1984. Pleading for a natural D/C-boundary. Cour. Forschungsinst. Senckenberg 67, 241–246.

Wang, K., Attrep Jr., M., Orth, C.J., 1993. Global iridium anomaly, mass extinction, and redox change at the Devonian–Carboniferous boundary. Geology 19, 776–779.

Wenzel, B., Lecuyer, C., Joachimski, M.M., 2000. Comparing oxygen isotope records of Silurian calcite and phosphate—$\delta^{18}O$ composition of brachiopods and conodonts. Geochim. Cosmochim. Acta 64, 1859–1872.

Xu, D.-Y., Yan, Z., Zhang, Q.-W., Shen, Z.-D., Sun, Y.-Y., Ye, L.-F., 1986. Significance of a $\delta^{13}C$ anomaly near the Devonian/Carboniferous boundary at the Muhua section, South China. Nature 321, 854–855.

Ziegler, W., Sandberg, C.A., 1984. *Palmatolepis*-based revision of upper part of standard Late Devonian conodont zonation. Spec. Pap. - Geol. Soc. Am. 196, 179–194.